

K.P. Singh
President and CEO
Holtec International

A.I. Soler
Chief Technology Officer
Holtec International

A Rational Procedure for Analyzing Flanged and Flued Expansion Joints

This paper presents a procedure for computing the axial stiffness of "formed head" type of expansion joints. The method given herein is an extension of the plate and shell theory adaptation of the "Kopp and Sayre method" first published by the authors in the text, Singh and Soler (1984). Arcturus Publishers. The approach suggested in this paper has been adopted by the Seventh Edition of the TEMA Standards.

1 Introduction

The subject of this paper is the so-called "formed head" type of expansion joint (Singh and Soler, 1984, p. 694). Such an expansion joint is typically made by forming a "flanged and flued head" out of a plate stock (Fig. 1). Two flanged and flued heads butt-welded together, as shown in Fig. 2, constitute a complete expansion joint. This joint is incorporated in the main shell of fixed tubular exchangers to impart a certain measure of axial flexibility to the shell, and thus help mitigate the stresses produced by difference in the length change of the shell and the tubes due to temperature and pressure loadings. The formed head expansion joint is the most common variety used in tubular heat exchangers, although the so-called "bellows type" is also occasionally used. The standards of the Expansion Joint Manufacturers Association (EJMA) (1980) gives rules for evaluating the stiffness of the "bellows type" of expansion joints. No such rules for designing the formed head expansion joint currently exist in any of the national codes or standards.

This glaring gap in the heat exchanger design codes has been recognized by both the relevant ASME code committees and the TEMA technical committee. Approximately five years ago, the Section VIII Division 1 working group on heat exchanger components of the ASME and TEMA organization's subcommittee on expansion joints started work on developing rules and guidelines for designing formed head expansion joints. The principal author of this paper, as a member of the latter committee, participated in the work on this subject until the end of 1986. The Seventh Edition of the TEMA Standards contains an extensive treatment on the expansion joint design problem based on the work reported in this paper. Indications are that the ASME working group, of which the co-author is an active member, will cease further rule-making on this subject in view of TEMA's initiative in this matter.

As for the TEMA Standards (1978), the rules for expansion joints will not come a day too soon. The formulas for designing fixed tubesheets occupy several pages in the standards

document, and make explicit reference to and use of the expansion joint stiffness (denoted as S_j in that document). Yet, the designer must look elsewhere for the method to compute S_j .

While the procedure for computing the expansion joint stiffness presented in this paper parallels TEMA's Seventh Edition, it does not entirely coincide with the final published version of the Seventh Edition of the TEMA Standards. The purpose of this paper is to merely present a rational basis for carrying out the stiffness computations, and to serve the role

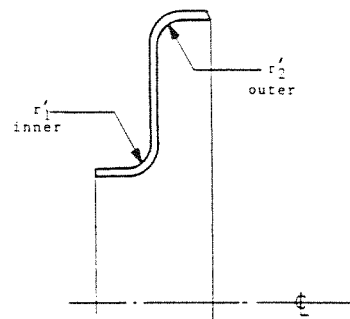


Fig. 1 Flanged and flued head

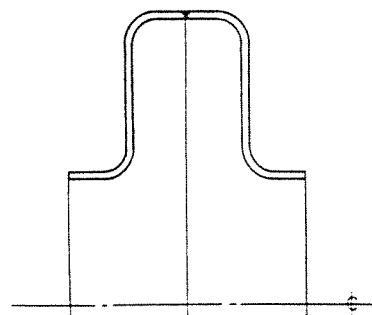


Fig. 2 Flanged and flued expansion joint

Contributed by the Pressure Vessels and Piping Division for publication in the JOURNAL OF PRESSURE VESSEL TECHNOLOGY. Manuscript received by the PVP Division, September 23, 1988; revised manuscript received July 17, 1990.

of the repository of the thought processes underlying the formulas in the standards.

The formulas evolved in this paper lend to expeditious computing on a personal computer. The application of a computer program based on this theory is also presented in this paper.

For reasons of time and space, this paper is confined to presenting the formulas to compute the expansion joint stiffness. The matter of the stresses in the expansion joint will be taken up in a future paper planned on this subject.

2 Prior Art

Kopp and Sayre (1952) are generally credited with the first comprehensive effort to determine the axial stiffness of "flanged only" joints analytically. They also conducted some experimental tests to verify their mathematical model. Their model is based on the following simplifying assumptions.

(a) The outer torus is replaced by an equivalent corner end. One-half of the meridian of the outer torus (total length $\pi r_2'/2$) is assigned to the outer plate and the other half is assigned to the outer shell. Figure 3(b) shows the idealized model.

(b) The annular plate is modeled by a unit width beam strip. Similarly, the structural characteristics of the outer shell are not modeled using classical thin shell equations. Instead an approximate relationship is used. However, the inner shell (heat exchanger main shell) is modeled using thin shell bending equations.

Despite the unevenness of their analytical premise, Kopp and Sayre obtained good agreement with their experimental data. The simplicity of their approach apparently sits well with the design community; their method is still specified as the standard design approach in numerous design specifications.

Another notable attempt to treat "flanged and flued expansion joint" is due to Wolf and Mains (1973). Wolf and Mains advocated a finite element solution of the axisymmetrically loaded expansion joint problem. Their method did not attract wide usage, although it is generally believed that the ascendance of purely numerical methods in design work is only a matter of time.

After considering the Kopp and Sayre solution, the TEMA technical committee decided to upgrade it by using classical plate and shell solutions in place of "beam" solutions. Such a solution is presented in Singh and Soler (1984). However, the treatment in that text suffers from the limitation of considering one standard expansion joint geometry. In practical ap-

plications, myriad variations on the standard flanged and flued configuration are employed. The task of the TEMA standards developers lay in generalizing the treatment of Singh and Soler (1984), while retaining its modeling assumptions, which are directly borrowed from Kopp and Sayre.

In the course of this effort towards generalization, the TEMA group proposed a generalized elemental shape which was given the euphemistic name "flexible shell element." In the next section, we will describe the geometry of "flexible shell element" and explain the modeling assumptions to simplify the mathematical problem.

3 Mathematical Model

The most general form of the flexible shell element is shown in Fig. 4. The following comments on the flexible shell element geometry will clarify the model:

(i) The flexible shell element is one half of a standard expansion joint. Two flexible elements together make a standard expansion joint, such as the one shown in Fig. 3(a).

(ii) The flexible shell element (FSE) may have tori at its small and large diameters. Setting the radius of a torus equal to zero simulates a corner joint.

(iii) The shells abutting the FSE at the inner and outer diameters may have different thicknesses and Young's moduli. Thus, attachment of the FSE to a relatively rigid member. For example, a tubesheet at the large diameter can be simulated by setting the Young modulus of the abutting outer shell very large.

(iv) The first step in the model simplification is to replace the circular segments with straights in the manner of Kopp and Sayre. The resulting idealized model has the appearance of Fig. 5. (The reader may refer to Singh and Soler (1984) for details.)

(v) In the next step, the composite shells located at radii a and b are replaced by an equivalent shell of thickness t_1 and t_2 , respectively, with modified flexural rigidities. Appendix A gives the necessary expressions for deriving the equivalent flexural rigidity of a composite shell. Thus, the flexible shell element is reduced to two concentric shells of radii a and b connected by an annular plate. The Young moduli of the three elements can be different.

The three elements of the flexible shell element can be characterized as follows:

Nomenclature

a, b, c, d = dimensionless quantities	r = generic notation for radius	
a, b = inner and outer radii of idealized flexible shell element, respectively	r_i = mean radius of shells ($i = 1, 2$)	ν = Poisson ratio
C_1, C_2 = constants of integration	r_1', r_2' = radii of tori (Fig. 1)	ζ = ratio of β_1 to β_2 ($\zeta = \beta_1/\beta_2$)
D = flexural rigidity	s = length of short shell (Fig. 8)	θ_i = rotation
E = Young's modulus	t = shell thickness	δ_i = radial (membrane) displacement (equation (12))
F = axial force per unit circumference	t_e = thickness of annular plate portion of expansion joint	Δ = determinant (equation (22))
G_1, G_2 = constants of integration	w = radial deflection	
K = stiffness of FSE (equation (24))	x_i = derivative terms (preceding equation (19))	
l_i = shell length term ($i = 1, 2$)	α_1, α_2 = defined in equation (33)	Subscripts
M_A = radially symmetric moment applied at location A	ϕ_1, ϕ_2 = defined in equation (33)	A = pertains to location A
	ψ_1, ψ_2 = defined in equation (33)	1 = short shell
	θ_A = rotation of meridian at location A	2 = long shell
		e = annular plate

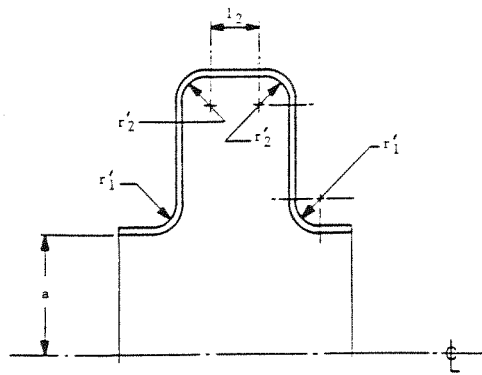


Fig. 3(a) Kopp and Sayre's model; actual geometry

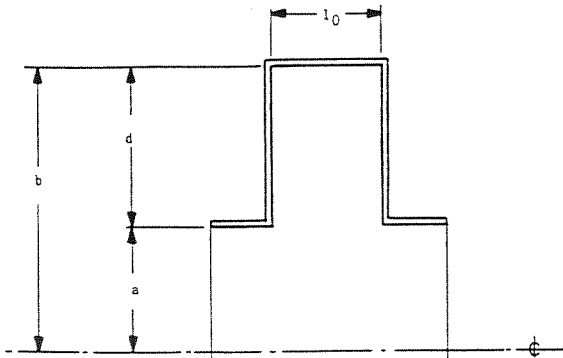


Fig. 3(b) Kopp and Sayre's model; idealized geometry

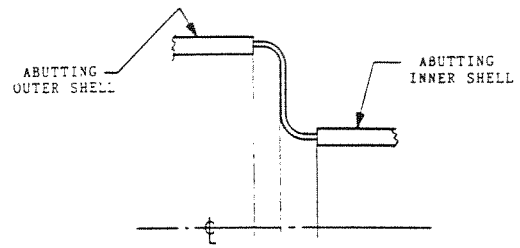


Fig. 4

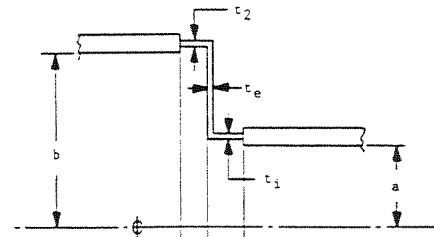


Fig. 5 Equivalent Kopp and Sayre model

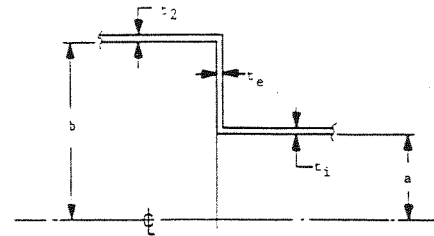


Fig. 6 Final idealized model

- (a) inner shell of thickness t_1 , equivalent Young's modulus E_1 , equivalent length l_1 and radius a ;
- (b) outer shell of thickness t_2 , equivalent Young's modulus E_2 , length l_2 , and radius b ;
- (c) annular plate of thickness t_e , inner and outer radii a and b , respectively.

The equivalent lengths l_1 and l_2 warrant further comment. For the inner shell l_1 should be taken sufficiently long such the edge effects (at the annular plate shell junction) die out. Taking $l_1 = 2.5 (at_1)^{1/2}$ will suffice, unless the shell is shorter, in which case the actual length should be used.

Similarly, the length l_2 is actual half-length of the top shell in the expansion joint. Within the framework of the foregoing assumptions, the expression for the axial stiffness can be derived in the manner described in Singh and Soler (1984). The essentials of the procedure are outlined in the forthcoming. We will first proceed to lay down the necessary interaction relations.

4 Interaction Relations

Figure 6 shows the free body representation of the idealized flexible shell element. Axial equilibrium yields

$$2\pi F_2 b = 2\pi F_{ax} a$$

$$\text{or} \quad F_2 = F_{ax} \frac{a}{b} \quad (1)$$

where F_{ax} is the axial load per unit circumference applied at the main shell. Our object is derive the expression for the separation of the joint due to the applied load, F_{ax} .

We now require the load/deflection relations for "short shell" and "annular plate" elements to assemble the stiffness equations.

(a) **Annular Plate.** The free body of the annular plate involves edge shear F_{ax} and edge moment M_1 at its inner cir-

cumference; and counterbalancing edge shear F_2 , and moment M_2 at its outer circumference. Referring to Singh and Soler (1984), the lateral deflection of a circle at radius r with respect to the outer edge is given by

$$w_e = M_1 g_1(r) + M_2 g_2(r) + F_{ax} f_1(r) \quad (2)$$

where

$$g_1(r) = \frac{1}{2} \frac{r^2 - b^2}{a^2 - b^2} \frac{a^2}{(1 + \nu) D_e} + \frac{a^2 b^2}{(a^2 - b^2)(1 - \nu) D_e} \ln \frac{r}{b} \quad (3)$$

$$g_2(r) = -\frac{1}{2} \frac{r^2 - b^2}{a^2 - b^2} \frac{b^2}{(1 + \nu) D_e} - \frac{a^2 b^2}{(a^2 - b^2)(1 - \nu) D_e} \ln \frac{r}{b} \quad (4)$$

$$f_1(r) = \frac{b^2 a}{4 D_e} \left\{ \left(1 - \frac{r^2}{b^2} \right) \left[\frac{3 + \nu}{2(1 + \nu)} + \frac{a^2}{a^2 - b^2} \ln \frac{a}{b} \right] + \frac{r^2}{b^2} \ln \frac{r}{b} - \frac{2a^2}{a^2 - b^2} \frac{1 + \nu}{1 - \nu} \ln \frac{a}{b} \ln \frac{r}{b} \right\} \quad (5)$$

where r is the radial coordinate and D_e represents the plate flexural rigidity.

$$D_e = \frac{E t_e^3}{12(1 - \nu^2)} \quad (6)$$

Differentiating

$$\frac{dg_1}{dr} = \frac{ra^2}{(a^2 - b^2)(1 + \nu)D_e} + \frac{a^2b^2}{(a^2 - b^2)(1 - \nu)D_e} \frac{1}{r}$$

$$\frac{dg_2}{dr} = -\frac{rb^2}{(a^2 - b^2)(1 + \nu)D_e} - \frac{a^2b^2}{(a^2 - b^2)(1 - \nu)D_e} \frac{1}{r}$$

$$\frac{df_1}{dr} = \frac{b^2a}{4D_e} \left\{ \frac{-2r}{b^2} \left[\frac{3 + \nu}{2(1 + \nu)} + \frac{a^2}{a^2 - b^2} \ln \frac{a}{b} \right] + \frac{2r}{b^2} \ln \frac{r}{b} + \frac{r}{b^2} - \frac{1}{r} \frac{2a^2}{a^2 - b^2} \frac{1 + \nu}{1 - \nu} \ln \frac{a}{b} \right\}$$
 (9)

We will need these expressions later in our work.

(b) Inner and Outer Shell. We shall use subscripts 1 and 2 to denote the inner and outer shell respectively. Thus, $F_i = F_{ax}$ is the axial load per unit circumference at the inner shell; and t_i , l_i , r_i , respectively, denote its thickness, effective length and mean radius.

Shell i is loaded with the edge moment M_i , edge shear Q_i and axial load F_i per unit circumference. We assume that its slope at the other end from the shell/annular plate junction (at distance l_i) is zero.

The radial displacement and slope at the junction are given by (Singh and Soler, 1984, p. 598).

$$w_i = \frac{-2Q_i\beta_i r_i^2}{E_i t_i} \chi_1(\alpha_i) + \frac{2M_i\beta_i^2 r_i^2}{E_i t_i} \chi_2(\alpha_i) + \delta_i$$
 (10)
$$\theta_i = \frac{-2Q_i\beta_i^3 r_i^2}{E_i t_i} \chi_2(\alpha_i) + \frac{4M_i\beta_i^3 r_i^2}{E_i t_i} \chi_3(\alpha_i)$$
 (11)

where

$$\delta_i = \frac{-\nu F_i r_i}{E_i t_i}$$
 (12)
$$\beta_i = \left[\frac{3(1 - \nu^2)}{r_i^2 t_i^2} \right]^{1/4}$$
 (13)
$$\alpha_i = \beta_i l_i / 2$$
 (14)
$$\chi_1 = \frac{\cosh 2\alpha_i + \cos 2\alpha_i}{\chi^*}$$
 (15a)
$$\chi_2 = (\sinh 2\alpha_i - \sin 2\alpha_i) / \chi^*$$
 (15b)
$$\chi_3 = (\cosh 2\alpha_i - \cos 2\alpha_i) / \chi^*$$
 (15c)
$$\chi^* = \sinh 2\alpha_i + \sin 2\alpha_i$$
 (15d)

Since $w_i \equiv 0$, we have

$$Q = \frac{M_i \beta_i \chi_2}{\chi_1} + \frac{E_i t_i \delta_i}{2\beta_i r_i^2 \chi_1}$$
 (16)

Substituting for e_i in equation (11) yields

$$e_i = y_i M_i - \frac{\beta_i \chi_2}{\chi_1} \delta_i$$
 (17)

where

$$y_i = \frac{4\beta_i^3 r_i^2}{E_i t_i} \chi_3 - \frac{2\beta_i^3 r_i^2 \chi_2^2}{E_i t_i \chi_1}$$
 (18)

Compatibility Relations. Requiring compatibility of slope at the junction of the two shells with the annular plate enables

us to evaluate the discontinuity moments M_1 and M_2 . For convenience, let us denote

$$x_1 = \frac{dg_1}{dr} \Big|_{r=r_1}; x_2 = \frac{dg_2}{dr} \Big|_{r=r_1}; x_3 = \frac{df_1}{dr} \Big|_{r=r_1}$$
 (7)
$$x_4 = \frac{dg_1}{dr} \Big|_{r=r_2}; x_5 = \frac{dg_2}{dr} \Big|_{r=r_2}; x_6 = \frac{df_1}{dr} \Big|_{r=r_2}$$
 (8)

Then, slope continuities at $r=r_1$ and $r=r_2$ produce the following algebraic equations for M_i and M_2 :

$$(x_1 - y_1)M_1 + x_2 M_2 = -x_3 F_1 - \beta_1 \delta_1$$

$$x_4 M_1 + (x_5 + y_2)M_2 = -x_6 F_1 + \frac{\beta_2 \chi_2}{\chi_1} \delta_2$$
 (19)

M_1 and M_2 readily follow from the foregoing in terms of F_1 ($= F_{ax}$)

$$M_1 = \frac{1}{\Delta} [(x_5 + y_2)(-F_{ax} x_3 - \beta_1 \delta_1) - x_2(-F_{ax} x_6 - \delta_2 \beta_2 \chi_2 / \chi_1)]$$
 (20)

$$M_2 = \frac{1}{\Delta} [(x_1 - y_1)(-F_{ax} x_6 - \beta_2 \chi_2 \delta_2 / \chi_1) - x_4(-F_{ax} x_3 - \beta_1 \delta_1)]$$
 (21)

where

$$\Delta = (x_1 - y_1)(x_5 + y_2) - x_2 x_4$$
 (22)

Having determined M_1 and M_2 , the spread of the flexible shell element is given by

$$\gamma = w_e \Big|_{r=r_1}$$
 (23)

The axial stiffness is simply

$$K = F_{ax} / \gamma$$
 (24)

5 Computer Code EXSTIFF

Computer code EXSTIFF implements the preceding analysis. The following studies illustrate the application of the code and confirm its validity.

We consider a series of cases wherein the Flexible Shell Element is made of a material of Young's modulus equal to 28 E + 06 psi (793000 MPa) throughout. The inner and outer torus radii are equal to 0.25 in. in all cases.

Table 1 gives the computed axial stiffness of the FSE using EXSTIFF. In the first five cases, the thickness of the main shell is set very large, and the thickness of its outer shell is set very small. Thus, in these cases, the FSE problem degenerates to that of an annular plate clamped at the inner circumference and free at the outer edge. The value of stiffness for this limiting case can be obtained using classical plate theory results. We note that the EXSTIFF solution is in remarkable agreement with the classical solution. The last column in the table gives the stiffness if the inner shell and outer shell thicknesses were equal to the annular plate thickness in the FSE.

Table 1 Validation studies of computer code EXSTIFF

Case no.	t_e (in.)	Inner radius (in.)	Outer radius (in.)	Stiffness EXSTIFF result	(lb/in.) classical solution	EXSTIFF solution for $t_i = t_2 = t_e$
1	0.25	24	30	97960	95316	377802
2	0.25	24	36	13685	13540	52772
3	0.4	24	36	56056	55531	216157
4	0.4	24	48	8908	8869	32786
5	0.4	16	48	3724	3721	12572
6	0.4	16	48	1068	1060	—
7	0.4	24	48	1171	1157	—
8	0.4	24	36	2719	2664	—
9	0.25	24	36	663	650	—
10	0.25	24	30	1472	1425	—

$$\frac{dg_1}{dr} = \frac{ra^2}{(a^2 - b^2)(1 + \nu)D_e} + \frac{a^2b^2}{(a^2 - b^2)(1 - \nu)D_e} \frac{1}{r}$$

$$\frac{dg_2}{dr} = -\frac{rb^2}{(a^2 - b^2)(1 + \nu)D_e} - \frac{a^2b^2}{(a^2 - b^2)(1 - \nu)D_e} \frac{1}{r}$$

$$\frac{df_1}{dr} = \frac{b^2a}{4D_e} \left\{ \frac{-2r}{b^2} \left[\frac{3 + \nu}{2(1 + \nu)} + \frac{a^2}{a^2 - b^2} \ln \frac{a}{b} \right] + \frac{2r}{b^2} \ln \frac{r}{b} + \frac{r}{b^2} - \frac{1}{r} \frac{2a^2}{a^2 - b^2} \frac{1 + \nu}{1 - \nu} \ln \frac{a}{b} \right\}$$
 (9)

We will need these expressions later in our work.

(b) Inner and Outer Shell. We shall use subscripts 1 and 2 to denote the inner and outer shell respectively. Thus, $F_i = F_{ax}$ is the axial load per unit circumference at the inner shell; and t_i , l_i , r_i , respectively, denote its thickness, effective length and mean radius.

Shell i is loaded with the edge moment M_i , edge shear Q_i and axial load F_i per unit circumference. We assume that its slope at the other end from the shell/annular plate junction (at distance l_i) is zero.

The radial displacement and slope at the junction are given by (Singh and Soler, 1984, p. 598).

$$w_i = \frac{-2Q_i\beta_i r_i^2}{E_i t_i} \chi_1(\alpha_i) + \frac{2M_i\beta_i^2 r_i^2}{E_i t_i} \chi_2(\alpha_i) + \delta_i$$
 (10)
$$\theta_i = \frac{-2Q_i\beta_i^2 r_i^2}{E_i t_i} \chi_2(\alpha_i) + \frac{4M_i\beta_i^3 r_i^2}{E_i t_i} \chi_3(\alpha_i)$$
 (11)

where

$$\delta_i = \frac{-\nu F_i r_i}{E_i t_i}$$
 (12)
$$\beta_i = \left[\frac{3(1 - \nu^2)}{r_i^2 t_i^2} \right]^{1/4}$$
 (13)
$$\alpha_i = \beta_i l_i / 2$$
 (14)
$$\chi_1 = \frac{\cosh 2\alpha_i + \cos 2\alpha_i}{\chi^*}$$
 (15a)
$$\chi_2 = (\sinh 2\alpha_i - \sin 2\alpha_i) / \chi^*$$
 (15b)
$$\chi_3 = (\cosh 2\alpha_i - \cos 2\alpha_i) / \chi^*$$
 (15c)
$$\chi^* = \sinh 2\alpha_i + \sin 2\alpha_i$$
 (15d)

Since $w_i \equiv 0$, we have

$$Q = \frac{M_i \beta_i \chi_2}{\chi_1} + \frac{E_i t_i \delta_i}{2\beta_i r_i^2 \chi_1}$$
 (16)

Substituting for e_i in equation (11) yields

$$e_i = y_i M_i - \frac{\beta_i \chi_2}{\chi_1} \delta_i$$
 (17)

where

$$y_i = \frac{4\beta_i^3 r_i^2}{E_i t_i} \chi_3 - \frac{2\beta_i^3 r_i^2 \chi_2^2}{E_i t_i \chi_1}$$
 (18)

Compatibility Relations. Requiring compatibility of slope at the junction of the two shells with the annular plate enables

us to evaluate the discontinuity moments M_1 and M_2 . For convenience, let us denote

$$x_1 = \frac{dg_1}{dr} \Big|_{r=r_1}; \quad x_2 = \frac{dg_2}{dr} \Big|_{r=r_1}; \quad x_3 = \frac{df_1}{dr} \Big|_{r=r_1}$$
 (7)
$$x_4 = \frac{dg_1}{dr} \Big|_{r=r_2}; \quad x_5 = \frac{dg_2}{dr} \Big|_{r=r_2}; \quad x_6 = \frac{df_1}{dr} \Big|_{r=r_2}$$
 (8)

Then, slope continuities at $r=r_1$ and $r=r_2$ produce the following algebraic equations for M_i and M_2 :

$$(x_1 - y_1)M_1 + x_2 M_2 = -x_3 F_1 - \beta_1 \delta_1$$

$$x_4 M_1 + (x_5 + y_2)M_2 = -x_6 F_1 + \frac{\beta_2 \chi_2}{\chi_1} \delta_2$$
 (19)

M_1 and M_2 readily follow from the foregoing in terms of F_1 ($= F_{ax}$)

$$M_1 = \frac{1}{\Delta} [(x_5 + y_2)(-F_{ax} x_3 - \beta_1 \delta_1) - x_2(-F_{ax} x_6 - \delta_2 \beta_2 \chi_2 / \chi_1)]$$
 (20)

$$M_2 = \frac{1}{\Delta} [(x_1 - y_1)(-F_{ax} x_6 - \beta_2 \chi_2 \delta_2 / \chi_1) - x_4(-F_{ax} x_3 - \beta_1 \delta_1)]$$
 (21)

where

$$\Delta = (x_1 - y_1)(x_5 + y_2) - x_2 x_4$$
 (22)

Having determined M_1 and M_2 , the spread of the flexible shell element is given by

$$\gamma = w_e \Big|_{r=r_1}$$
 (23)

The axial stiffness is simply

$$K = F_{ax} / \gamma$$
 (24)

5 Computer Code EXSTIFF

Computer code EXSTIFF implements the preceding analysis. The following studies illustrate the application of the code and confirm its validity.

We consider a series of cases wherein the Flexible Shell Element is made of a material of Young's modulus equal to 28 E + 06 psi (793000 MPa) throughout. The inner and outer torus radii are equal to 0.25 in. in all cases.

Table 1 gives the computed axial stiffness of the FSE using EXSTIFF. In the first five cases, the thickness of the main shell is set very large, and the thickness of its outer shell is set very small. Thus, in these cases, the FSE problem degenerates to that of an annular plate clamped at the inner circumference and free at the outer edge. The value of stiffness for this limiting case can be obtained using classical plate theory results. We note that the EXSTIFF solution is in remarkable agreement with the classical solution. The last column in the table gives the stiffness if the inner shell and outer shell thicknesses were equal to the annular plate thickness in the FSE.

Table 1 Validation studies of computer code EXSTIFF

Case no.	t_e (in.)	Inner radius (in.)	Outer radius (in.)	Stiffness EXSTIFF result	(lb/in.) classical solution	EXSTIFF solution for $t_i = t_2 = t_e$
1	0.25	24	30	97960	95316	377802
2	0.25	24	36	13685	13540	52772
3	0.4	24	36	56056	55531	216157
4	0.4	24	48	8908	8869	32786
5	0.4	16	48	3724	3721	12572
6	0.4	16	48	1068	1060	---
7	0.4	24	48	1171	1157	---
8	0.4	24	36	2719	2664	---
9	0.25	24	36	663	650	---
10	0.25	24	30	1472	1425	---

The last five cases in Table 1 correspond to the reverse situation wherein the inner shell is very thin and the outer shell is very thick. The classical solution results for this case also are seen to agree extremely well with EXSTIFF.

6 Closure

A computationally expedient method to evaluate the axial stiffness of "Flexible Shell Elements" has been presented. The computer code EXSTIFF based on the theory of this paper has been validated by running test cases of limiting flexible shell element geometries which can be checked out against classical solutions. The general framework of the method presented herein has been adopted by the Seventh Edition of the TEMA Standards.

Acknowledgments

The principal author is grateful to his former TEMA colleagues, Messrs. Tom Lodes, John McCutchen and Tom Spencer for their many insightful contributions in developing the theory of this paper.

References

- Singh, K. P., and Soler, A. I., 1984, *Mechanical Design of Heat Exchangers and Pressure Vessel Components*, Arcturus Publishers, Cherry Hill, N.J.
- Anono, 1980, *Standards of the Expansion Joint Manufacturers Association*, EJMA, Inc., Tarrytown, N.Y.
- Anono, 1978, *Standards of Tubular Exchanger Manufacturers Association*, TEMA, Inc., Sixth Edition, Tarrytown, N.Y.
- Kopp, S., and Sayre, M. F., 1952, "Expansion Joints for Heat Exchangers," ASME Winter Annual Meeting, N.Y.
- Wolf, L. J., and Mains, R. M., 1973, "The Stress Analysis of Heat Exchangers in the Elastic Range," *ASME Journal of Engineering for Industry*, pp. 145-150.

APPENDIX A

In this appendix, we present the necessary analysis to obtain the algebraic expressions required to define the "equivalent rigidity" of a "composite shell segment." The composite shell consists of a short shell of length s and thickness t_1 attached (integrally welded) to a "long" shell of thickness t_2 . The attachment location is hereafter referred to as the junction. Both shells have a common mean radius r . For our purposes here, the term "rigidity" means the ratio of a symmetrically applied moment M , to the resulting edge rotation of the generator, the former applied along with the requisite radial shear to maintain zero radial displacement at the location of moment application. In other words, the rigidity K is defined as

$$K = \frac{M_A}{\theta_A} \Big|_{w_A=0} \quad (25)$$

where M , θ , and w denote the applied radial moment, rotation and radial displacement, respectively. The subscript A indicates that those quantities pertain to location A (in Fig. 7). Our final object is to obtain the expression for the equivalent rigidity multiplier, e , which is defined as the ratio of the rigidity of a composite shell illustrated in Fig. 8 to that of a single "long" shell of constant thickness t_1 . The analysis utilizes classical thin shell theory, which is quite appropriate since expansion joints, by their very function, must belong in the "thin shell" category.

The equation for radially symmetric deformation of a cylindrical shell is well documented in the literature (Singh and Soler, 1984, pp. 1024-1035).

$$D \nabla^4 w = p(x) \quad (26)$$

where the flexural rigidity, D , is defined as

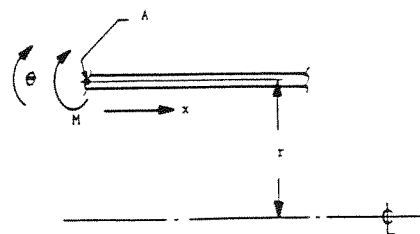


Fig. 7 Thin shell of radius r and thickness t under edge moment, and a prescribed zero edge radial displacement

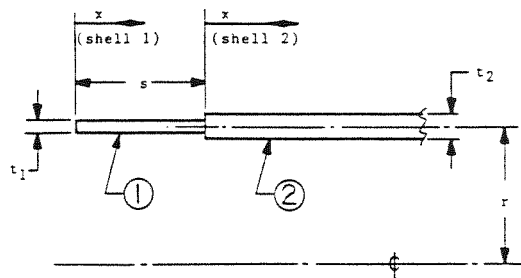


Fig. 8 Composite shell

$$D = \frac{Et^3}{12(1-\nu^2)} \quad (27)$$

The solution of equation (26) is given in terms of four undetermined constants of integration, C_1 , C_2 , G_1 and G_2 . In the absence of any distributed loadings, the particular solution is identically zero. We have

$$w = C_1 e^{\beta x} \cos \beta x + C_2 e^{\beta x} \sin \beta x + G_1 e^{-\beta x} \cos \beta x + G_2 e^{-\beta x} \sin \beta x \quad (28)$$

The expression for the slope moment and shear are obtained by successive differentiations.

$$\theta = \frac{-dw}{dx} = -\beta e^{\beta x} [C_1 (\cos \beta x - \sin \beta x) + C_2 (\cos \beta x + \sin \beta x)] + \beta e^{-\beta x} [G_2 (\cos \beta x - \sin \beta x) - \beta G_1 e^{-\beta x} (\cos \beta x + \sin \beta x)] \quad (29)$$

$$M = D \frac{d^2 w}{dx^2} = 2\beta^2 D [e^{\beta x} (C_2 \cos \beta x - C_1 \sin \beta x) + e^{-\beta x} (G_1 \sin \beta x - G_2 \cos \beta x)] \quad (30)$$

$$Q = \frac{dM}{dx} = 2\beta^3 D [e^{\beta x} \{ C_2 (\cos \beta x - \sin \beta x) - C_1 (\sin \beta x + \cos \beta x) \} + e^{-\beta x} \{ G_1 (\cos \beta x - \sin \beta x) + G_2 (\sin \beta x + \cos \beta x) \}] \quad (31)$$

The term β in the foregoing equations is termed the "attenuation coefficient," and is defined as

$$\beta = \left[\frac{3(1-\nu^2)}{r^2 t^2} \right]^{1/4} \quad (32)$$

Referring to the composite shell in Fig. 8, we will refer to the short shell as shell 1, and the long shell as shell 2. All variables and parameters are appended subscripts 1 or 2 indicating the shell they pertain to. For example, t_1 denotes thickness of shell 1, β_2 denotes the attenuation coefficient of shell 2.

In what follows, we will use certain symbols to denote frequently occurring grouping of terms. These are

$$e^{\beta_1 s} \cos \beta_1 s = \phi_1 \quad (33a)$$

$$e^{\beta_1 s} \sin \beta_1 s = \phi_2 \quad (33b)$$

$$e^{-\beta_1 s} \cos \beta_1 s = \psi_1 \quad (33c)$$

$$e^{-\beta_1 s} \sin \beta_1 s = \psi_2 \quad (33d)$$

$$\beta_1/\beta_2 = \xi \quad (33e)$$

$$\frac{\beta_1^2 D_1}{\beta_2^2 D_2} = \alpha_1; \quad \frac{\beta_1^3 D_1}{\beta_2^3 D_2} = \alpha_2 \quad (33f)$$

The solution for the radial displacement of shell i is written following equation (28)

$$w_i = C_{1i} e^{\beta_i x} \cos \beta_i x + c_{2i} e^{\beta_i x} \sin \beta_i x + G_{1i} e^{-\beta_i x} \cos \beta_i x + G_{2i} e^{-\beta_i x} \sin \beta_i x \quad i = 1, 2 \quad (34)$$

where the x coordinate for each shell begins at its left end in Fig. 8.

The eight constants of integration, C_{1i} , C_{2i} , etc., are solved for by using boundary and interface conditions. The detailed procedure is outlined below. Since shell 2 is infinitely long, finiteness of deflection as $x \rightarrow \infty$, requires that $C_{12} = C_{22} = 0$. This eliminates two integration constants from further algebra.

Continuity of slope at the junction between the shell 1 and shell 2 requires that

$$\left. \frac{dw_1}{dx} \right|_{x=s} = \left. \frac{dw_2}{dx} \right|_{x=0} \quad (35)$$

this leads to (using equation (29))

$$\beta_2 (-G_{12} + G_{22}) = \beta_1 \{ C_{11} (\phi_1 - \phi_2) + C_{21} (\phi_1 + \phi_2) - G_{11} (\psi_1 + \psi_2) + G_{21} (\psi_1 - \psi_2) \} \quad (36)$$

$$\text{or } G_{22} = C_{11} \{ \phi_1 (1 + \xi) - \zeta \phi_2 \} + C_{21} \{ (1 + \xi) \phi + \zeta \phi_1 \} + G_{11} \{ \psi_1 (1 - \xi) - \psi_2 \zeta \} + G_{21} \{ \psi_2 (1 - \xi) + \xi \psi_1 \} \quad (37)$$

Equating the externally applied moment M and shear Q to the internal moments and shear in shell 1, respectively, yields (from equation (30))

$$M = 2\beta_1^2 D_1 (C_{21} - G_{21}) \quad (38)$$

or

$$M' = C_{21} - G_{21}$$

where

$$M' = M / 2\beta_1^2 D_1 \quad (39)$$

and

$$Q = 2\beta_1^3 D_1 (C_{21} - C_{11} + G_{11} + G_{21}) \quad (40)$$

or

$$Q' = C_{21} - C_{11} + G_{11} + G_{21}$$

where

$$Q' = Q / 2\beta_1^3 D_1 \quad (41)$$

Therefore,

$$C_{21} = M' + G_{21}$$

and

$$C_{11} = M' - Q' + 2G_{21} + G_{11} \quad (42)$$

Next, we utilize displacement continuity at the junction to write another algebraic relationship between the integration constants.

$$w_1 \Big|_{x=s} = w_2 \Big|_{x=0} \quad (43)$$

$$\text{or } C_{11} \phi_1 + C_{21} \phi_2 + G_{11} \psi_1 + G_{21} \psi_2 = G_{12}$$

Substituting out C_{11} and C_{21} in the foregoing equations, we have

$$G_{12} = a_1 G_{21} + b_1 G_{11} + d_1 \quad (44)$$

where

$$a_1 = 2\phi_1 + \phi_2 + \psi_2 \quad (45a)$$

$$b_1 = \phi_1 + \psi_1 \quad (45b)$$

$$d_1 = (M' - Q') \phi_1 + M' \phi_2 \quad (45c)$$

Similarly, C_{11} and C_{21} can be substituted out from equation (37), leading to (after some algebra)

$$G_{22} = a_2 G_{21} + b_2 G_{11} + d_2 \quad (46)$$

where

$$a_2 = \phi_1 (2 + 3\xi) + \phi_2 (1 - \xi) + \xi \psi_1 + (1 - \xi) \psi_2 \quad (47a)$$

$$b_2 = \phi_1 (1 + \xi) - \xi \phi_2 + \psi_1 (1 - \xi) - \xi \psi_2 \quad (47b)$$

$$d_2 = M' \{ \phi_1 (1 + 2\xi) + \phi_2 \} - Q' \{ \phi_1 (1 + \xi) - \xi \phi_2 \} \quad (47c)$$

The last two required relationships follow from moment and shear continuity at the junction. Moment continuity yields

$$-2\beta_2^2 D_2 G_{22} = 2\beta_1^2 D_1 [-C_{11} \phi_2 + C_{21} \phi_1 + G_{11} \psi_2 - G_{21} \psi_1]$$

making the necessary substitutions for C_{11} , C_{21} and M_{22} from the foregoing equations, and rearranging terms gives the algebraic equation relating G_{21} and G_{11} . We obtain

$$a_3 G_{21} + b_3 G_{11} = d_3 \quad (48)$$

where

$$a_3 = a_2 - 2\alpha_1 \phi_2 + \alpha_1 \phi_1 - \alpha_1 \psi_1 \quad (49a)$$

$$b_3 = b_2 - \alpha_1 \phi_2 + \alpha_1 \psi_2 \quad (49b)$$

$$d_3 = -d_2 + \alpha_1 \phi_2 (M' - Q') - \alpha_1 M' \phi_1 \quad (49c)$$

Similarly, shear continuity is invoked to give

$$2D_1 \beta_1^3 [-C_{11} (\phi_1 + \phi_2) + C_{21} (\phi_1 - \phi_2) + G_{11} (\psi_1 - \psi_2) + G_{21} (\psi_1 + \psi_2)] = 2D_2 \beta_2^3 [G_{12} + G_{22}]$$

Proceeding as before, we obtain another linear algebraic relationship between G_{21} and G_{11}

$$a_4 G_{21} + b_4 G_{11} = d_4 \quad (50)$$

where

$$a_4 = \alpha_2 (-\phi_1 - 3\phi_2 + \psi_1 + \psi_2) - a_1 - a_2 \quad (51a)$$

$$b_4 = \alpha_2 (-\phi_1 - \phi_2 + \psi_1 - \psi_2) - b_1 - b_2 \quad (51b)$$

$$d_4 = 2\alpha_2 M' \phi_2 - \alpha_2 (\phi_1 + \phi_2) Q' + d_1 + d_2 \quad (51c)$$

The expressions for G_{21} and G_{11} are now obtained by solving the two equations (48) and (50). We obtain

$$G_{21} = b'_4 d_3 - b'_3 d_4 \quad (52a)$$

$$G_{11} = a'_3 d_4 - a'_4 d_3 \quad (52b)$$

where

$$b'_4 = b_4 / \Delta, \quad b'_3 = b_3 / \Delta, \quad a'_4 = a_4 / \Delta, \quad a'_3 = a_3 / \Delta \quad (53a)$$

$$\text{and } \Delta = a_3 b_4 - b_3 a_4 \quad (53b)$$

The condition that $w_A = 0$ enables us to express the shear Q in terms of the applied moment M . Since

$$w_1 \Big|_{x=0} = 0 \text{ implies that}$$

$$C_{11} + G_{11} = 0$$

Recalling the expression for C_{11} from equation (42) leads to

$$M' - Q' + 2G_{21} + 2G_{11} = 0 \quad (54)$$

Next, G_{21} and G_{11} are substituted out using equation (52); we have

$$M' - Q' + 2(b'_4 - a'_4) d_3 + 2(a'_3 - b'_3) d_4 = 0$$

The expressions for d_3 (equation (49)), and d_4 (equation (51)) can now be used to obtain the direct relationship between M and Q . Omitting the intermediate algebra, we get

$$Q' = \Lambda M' \quad (55)$$

where

$$\Lambda = \frac{1 + 2(b'_4 - a'_4) \{ \phi_2(\alpha_1 - 1) - \phi_1(1 + \alpha_1 + 2\xi) + 4(a'_3 - b'_3) \{ \phi_1(1 + \xi) + \phi_2(1 + \alpha_2) \} }{1 + 2(b'_4 - a'_4) \{ \phi_2(\alpha_1 - \xi) - \phi_1(1 + \xi) \} + 2(a'_3 - b'_3) \{ \phi_1(2 + \xi + \alpha_2) + \phi_2(\alpha_2 - \xi) \}} \quad (56)$$

Reverting back to equation (52), we have

$$G_{21} = b'_4 d_3 - b'_3 d_4$$

Substituting for d_3 and d_4 from the foregoing, and using equation (55), gives

$$G_{21} = \tau M' \quad (57)$$

where

$$\begin{aligned} \tau = & b'_4 \{ \phi_2(\alpha_1 - 1) - \phi_1(1 + \alpha_1 + 2\xi) \\ & - \Lambda \{ (\alpha_1 + \xi) \phi_2 - \phi_1(1 + \xi) \} \\ & - b'_3 \{ 2\phi_1(1 + \xi) + 2\phi_2(1 + \alpha_2) \\ & - \Lambda \{ \phi_1(2 + \xi + \alpha_2) + \phi_2(\alpha_2 - \xi) \} \} \end{aligned} \quad (58)$$

We now have all necessary equations to obtain e . For this, we write the expression for θ_A (using equation (29))

$$\begin{aligned} \theta_A = & \beta_1 (C_{11} + C_{21} - G_{11} + G_{21}) \\ = & \beta_1 (2M' - Q' + 4G_{21}) \end{aligned} \quad (59)$$

Q' and G_{21} are substituted out using equations (55) and (57), respectively, resulting in

$$\begin{aligned} \theta_A = & \beta_1 M' (2 - \Lambda + 4\tau) \\ \text{or} \quad \frac{M}{\theta_A} = & \frac{-2\beta_1 D_1}{2 - \Lambda + 4\tau} = K_e \end{aligned} \quad (60)$$

The rigidity of an infinitely long shell ($s = \infty$) is

$$K_1 = -2\beta_1 D_1$$

Therefore, the equivalent rigidity multiplier is

$$\begin{aligned} e = & K_e / K_1 \\ \text{or} \quad e = & - \frac{1}{2 - \Lambda + 4\tau} \end{aligned} \quad (61)$$

It can be readily shown that e is a function of the dimensionless quantities (E_1/E_2) , (t_1/t_2) and $s/(rt_1)^{1/2}$.